Supplement of Atmos. Chem. Phys., 21, 14851–14869, 2021
https://doi.org/10.5194/acp-21-14851-2021-supplement

Atmospheric Chemistry and Physics
Open Access
EGU

Supplement of

Sources of black carbon at residential and traffic environments obtained by two source apportionment methods

Sanna Saarikoski et al.

Correspondence to: Sanna Saarikoski (sanna.saarikoski@fmi.fi)

Supplemental material

Table S1. The contribution of rBC (the sum of C_2^+, C_3^+ and C_4^+) to the mass spectra of the PMF factors at the residential site.

PMF factor	3 factors	4 factors	5 factors
HOA	0.067	0.049	0.060
BBOA	0.077	0.090	0.079
LV-OOA	0.011	0.017	0.084
SV-OOA		0.041	0.022
LV-OOA-LRT			0.014

Table S2. The contribution of rBC (the sum of C_2^+, C_3^+ and C_4^+) to the mass spectra of the PMF factors at the street canyon site.

PMF factor	3 factors	4 factors	5 factors
HOA	0.139	0.142	0.142
BBOA	0.030	0.011	0.012
LV-OOA	0.086	0.077	0.081
SV-OOA		0.079	0.075
CoOA			0.047

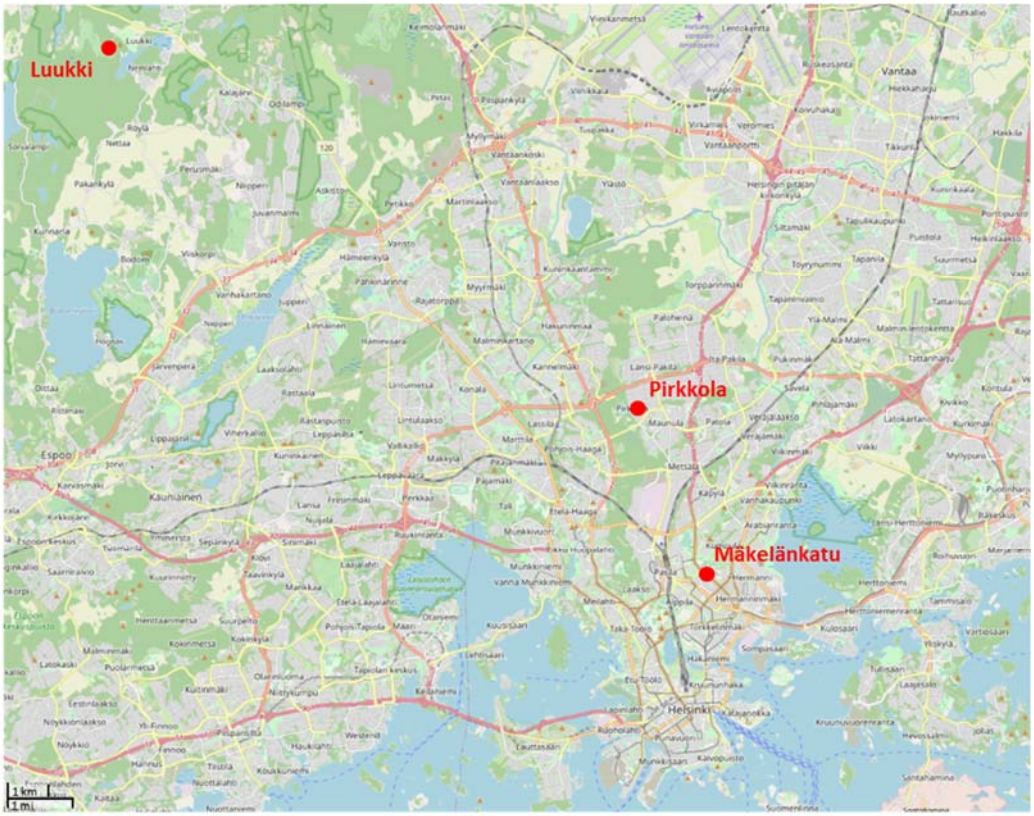

Figure S1. The locations of the measurement stations in the Helsinki metropolitan area; Mäkelänkatu street canyon supersite, Pirkkola residential area and Luukki regional background. Background map © OpenStreetMap contributors 2021. Distributed under the Open Data Commons Open Database License (ODbL) v1.0.".

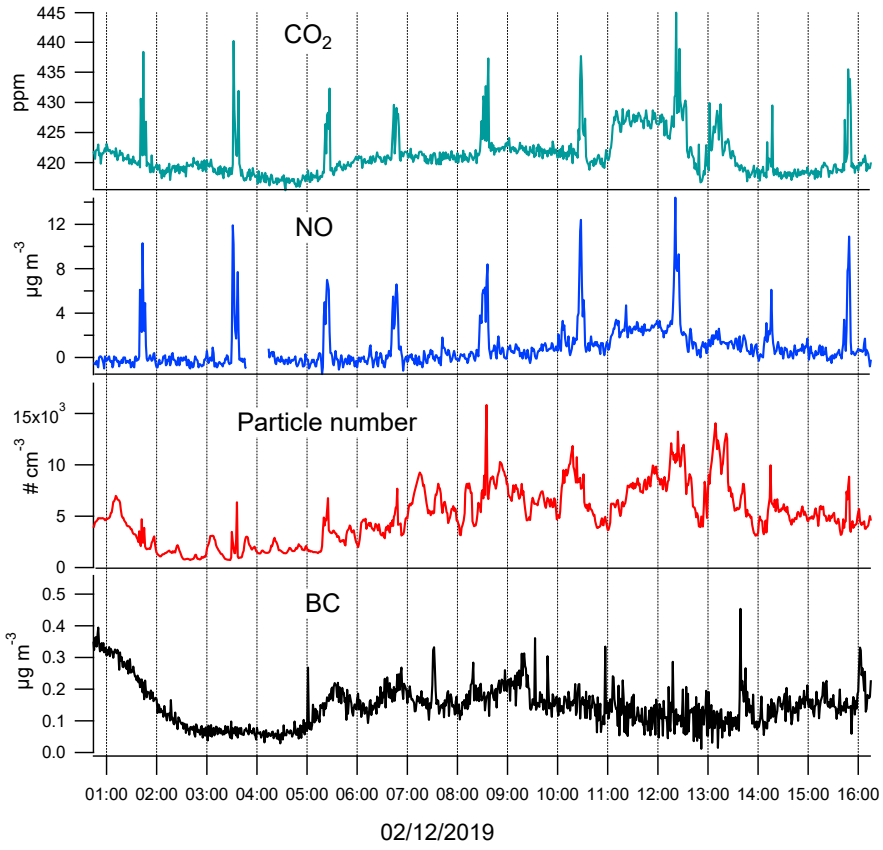

Figure S2. Example of the emissions from oil burning at the residential site. Oil burning emissions can be seen with sharp peaks (~10 minutes) especially for CO_2 and NO. Particle number concentration (>5 nm particles) was measured with the Condensation Particle Counter A20 (Airmodus, Helsinki, Finland).

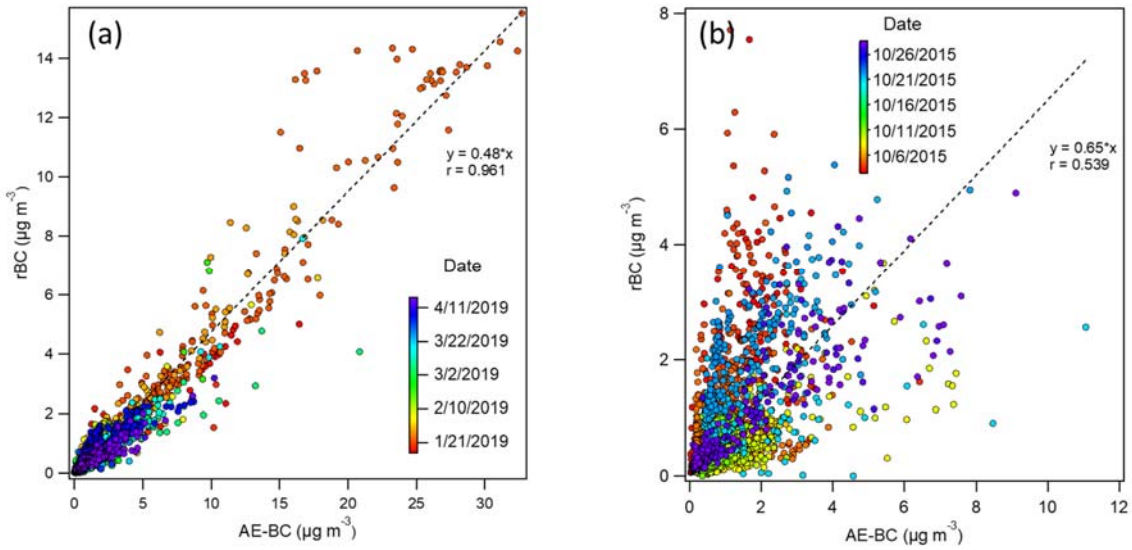

Figure S3. Comparison of BC from the SP-AMS (rBC) with BC from the aethalometer (AE) at the residential site (a) and street canyon (b). 10-min (a) and 5-min (b) time resolution. Dotted lines show linear fit.

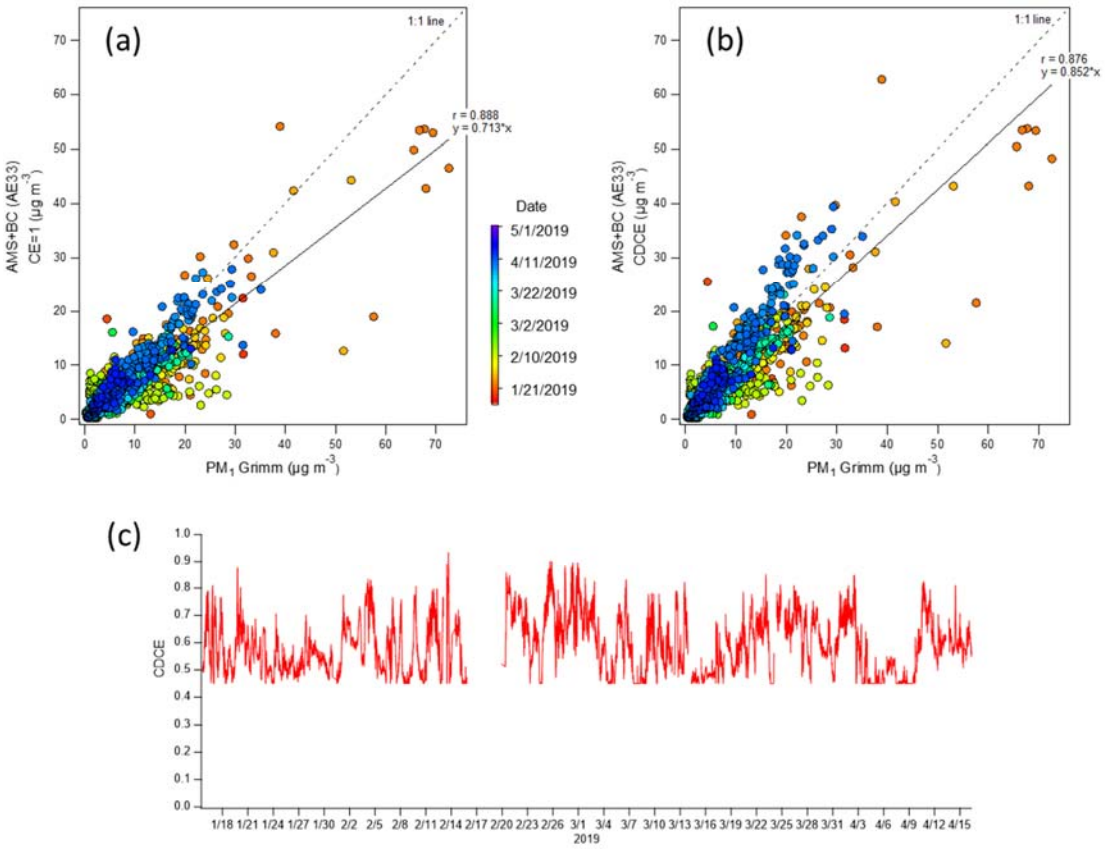

Figure S4. Comparison of the sum of the SP-AMS species (excluding rBC) and BC from the aethalometer with PM_1 from Grimm with CE=1 (a), with composition dependent collection efficiency (CDCE) (b), and the time series of CDCE (c) at the residential site. 1-hour (a-b) and 10-min (c) time resolution.

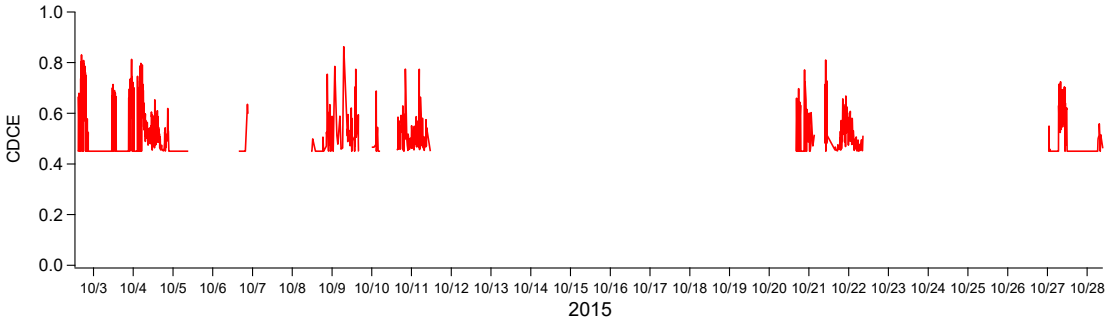

Figure S5. Time series of the composition dependent collection efficiency (CDCE) at the street canyon. 5-min time resolution.

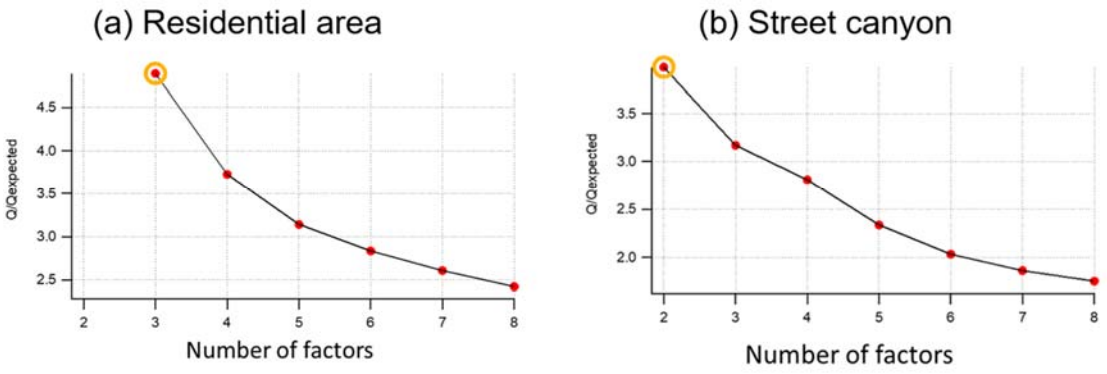

Figure S6. $Q/Q_{expected}$ for the PMF solutions of 2–8 factors for the data measured at the residential area (a) and street canyon (b). For the residential site, two-factor solution was inconclusive.

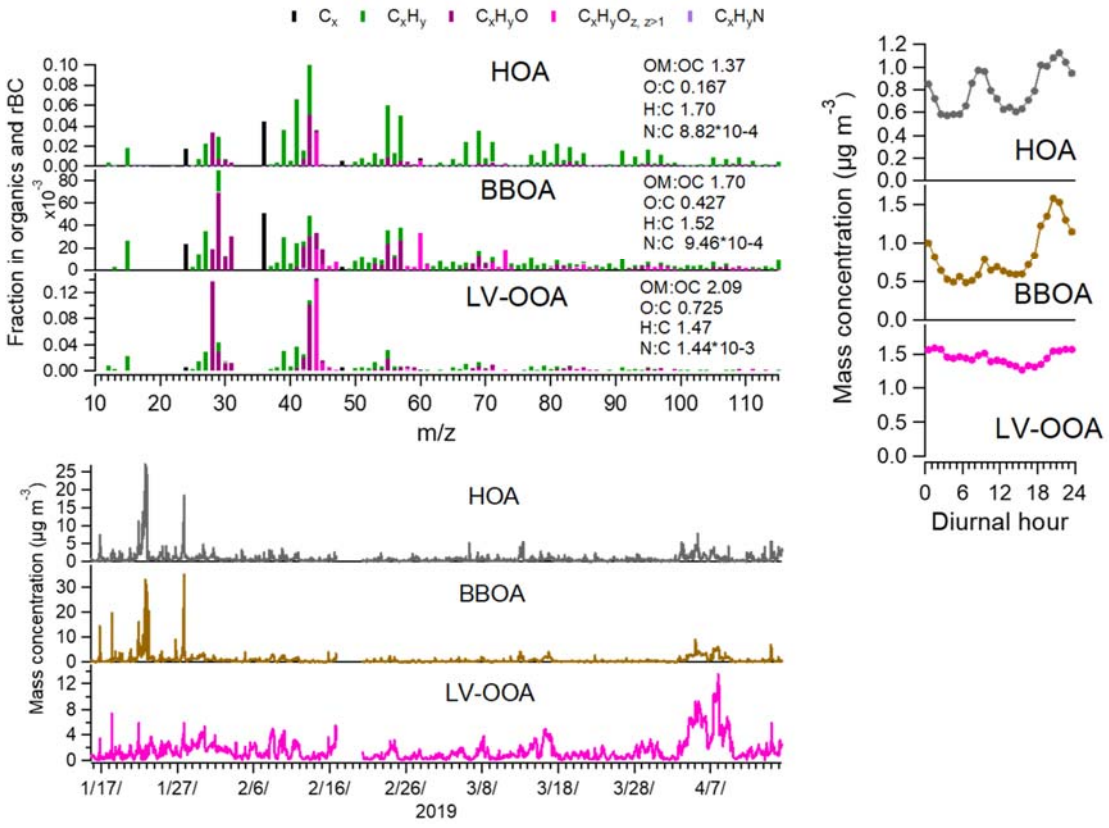

Figure S7. Mass spectra, times series and campaign-average diurnal trends for the three factor PMF solution for organics and rBC at the residential site. Elemental ratios (OM:OC, O:C, H;C and N:C) were calculated to organic mass spectra excluding rBC fragments. Colors in the mass spectra represent different types of organic fragments.

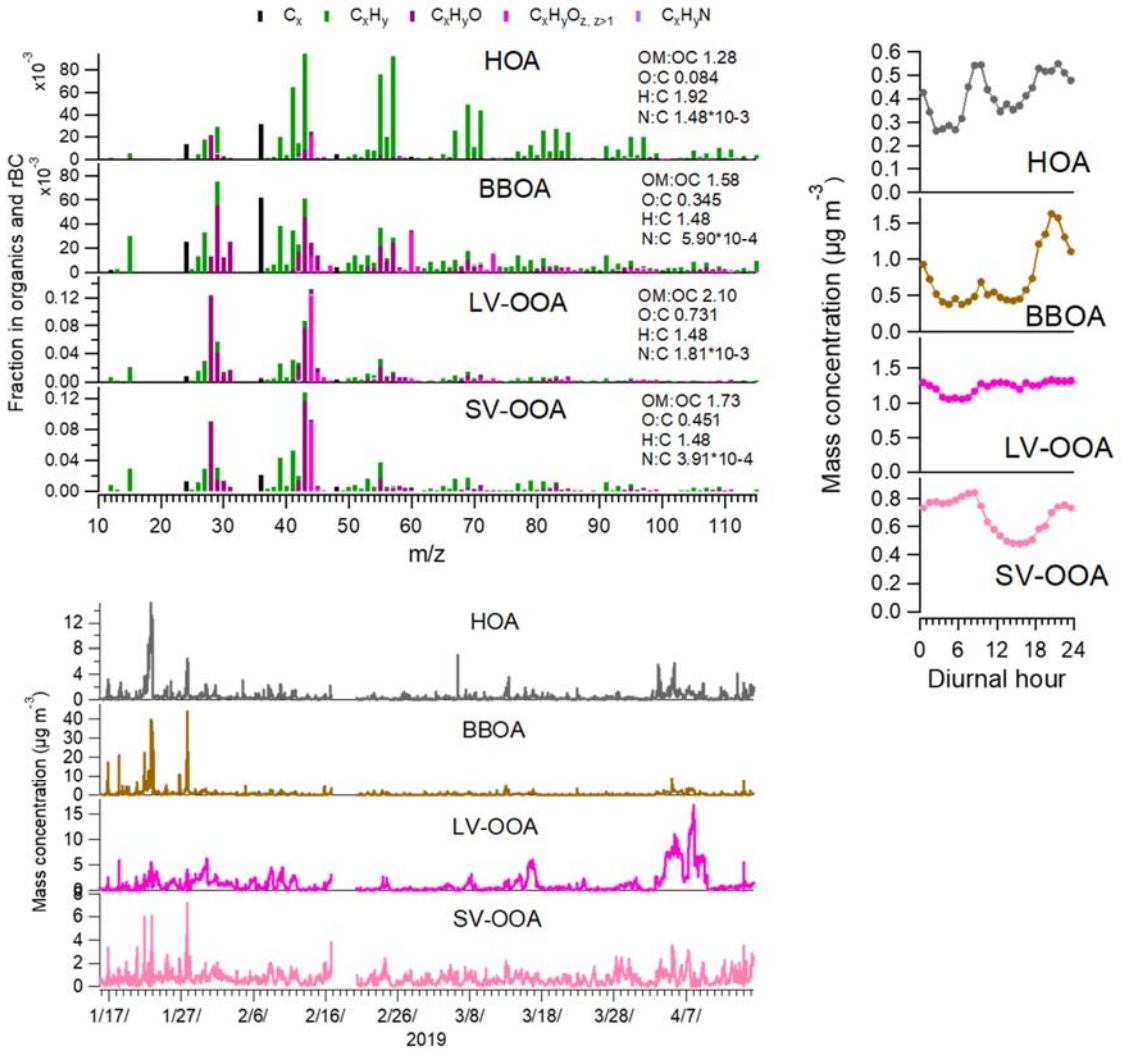

Figure S8. Mass spectra, times series and campaign-average diurnal trends for the four factor PMF solution for organics and rBC at the residential site. Elemental ratios (OM:OC, O:C, H;C and N:C) were calculated to organic mass spectra excluding rBC fragments. Colors in the mass spectra represent different types of organic fragments.

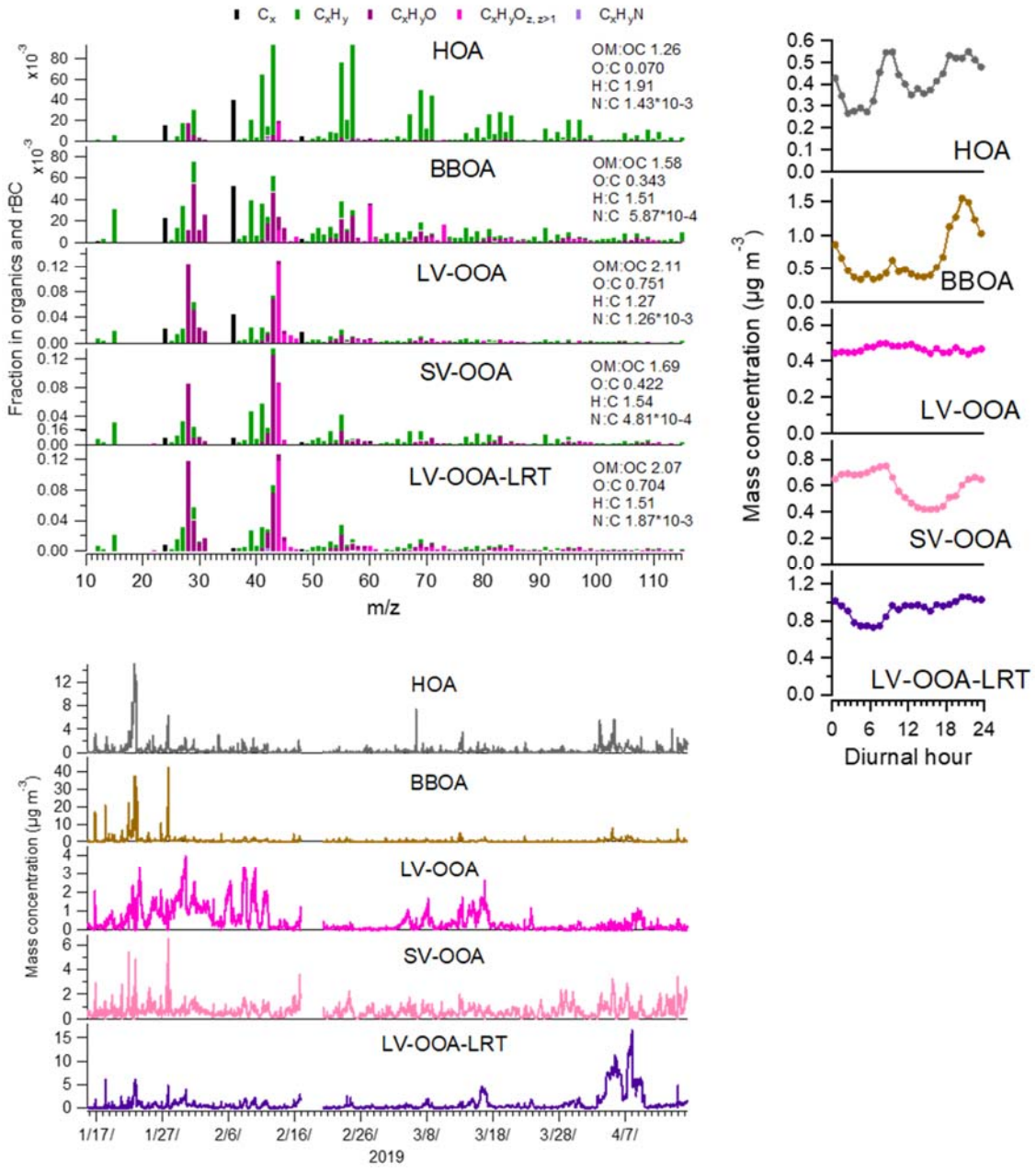

Figure S9. Mass spectra, times series and campaign-average diurnal trends for the five factor PMF solution for organics and rBC at the residential site. Elemental ratios (OM:OC, O:C, H;C and N:C) were calculated to organic mass spectra excluding rBC fragments. Colors in the mass spectra represent different types of organic fragments.

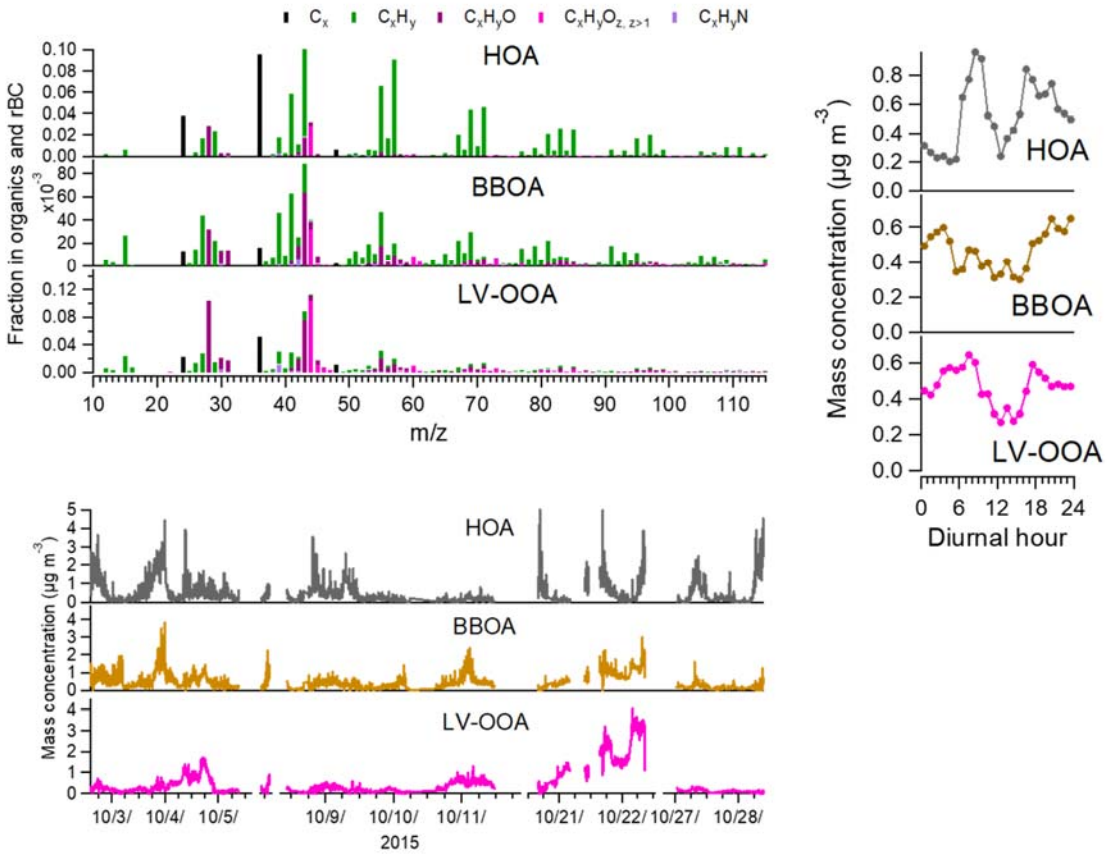

Figure S10. Mass spectra, times series and campaign-average diurnal trends for the three factor PMF solution for organics and rBC at the street canyon. Elemental ratios were not calculated due to the exclusion of CHO^+ from the input matrix. Colors in the mass spectra represent different types of organic fragments.

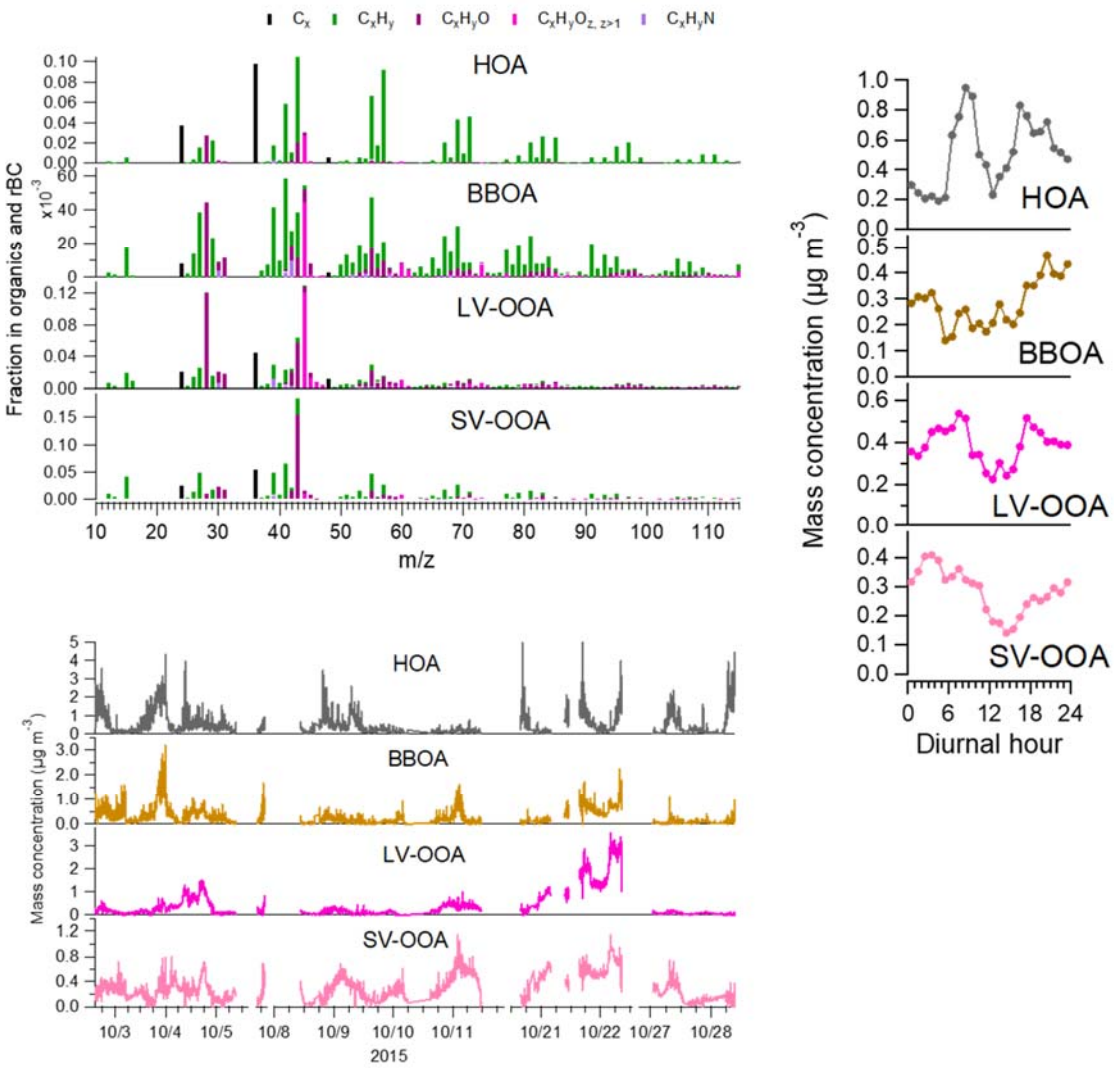

Figure S11. Mass spectra, times series and campaign-average diurnal trends for the four factor PMF solution for organics and rBC at the street canyon. Elemental ratios were not calculated due to the exclusion of CHO^+ from the input matrix. Colors in the mass spectra represent different types of organic fragments.

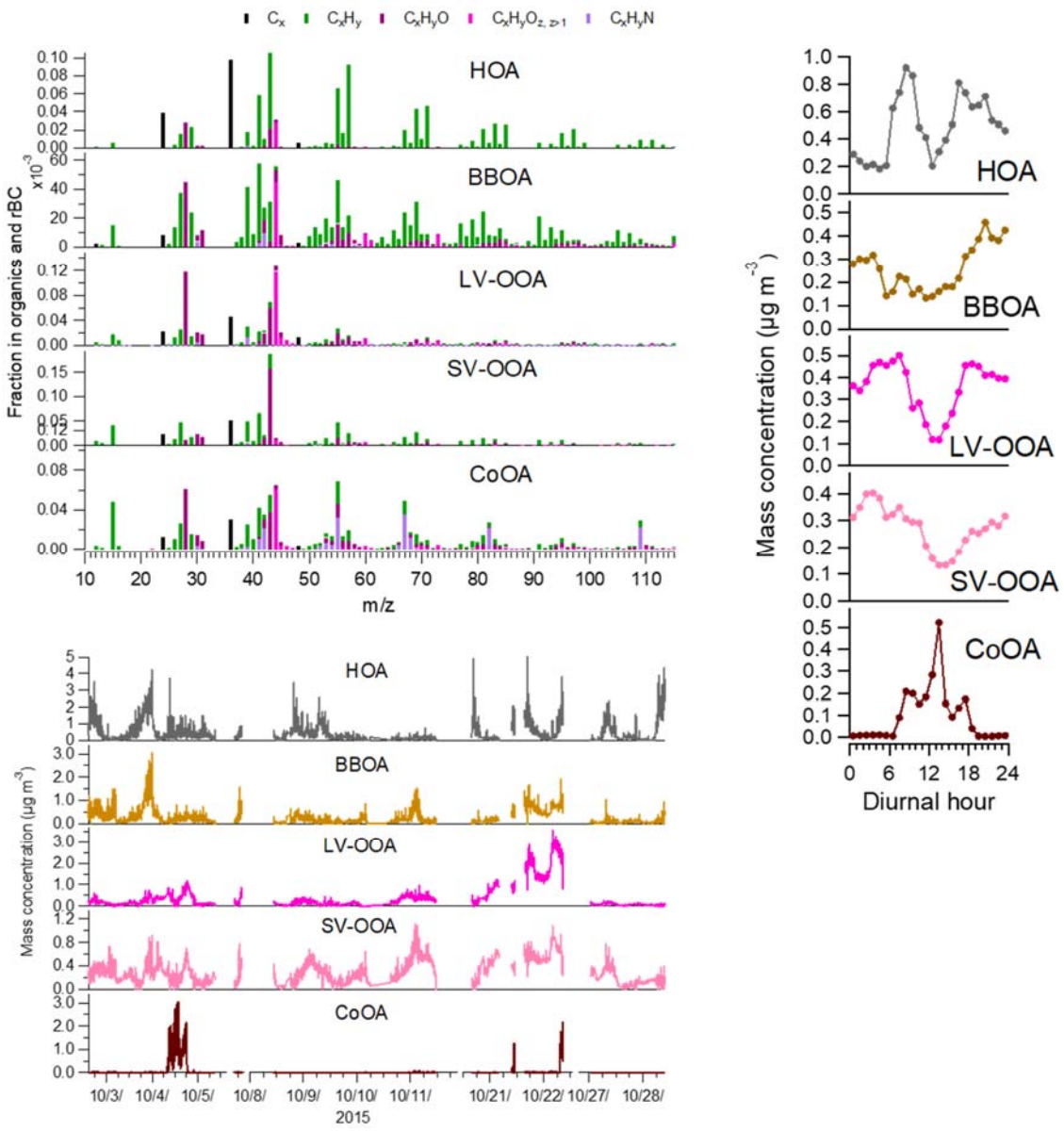

Figure S12. Mass spectra, times series and campaign-average diurnal trends for the five factor PMF solution for organics and rBC at the street canyon. Elemental ratios were not calculated due to the exclusion of CHO^+ from the input matrix. Colors in the mass spectra represent different types of organic fragments.

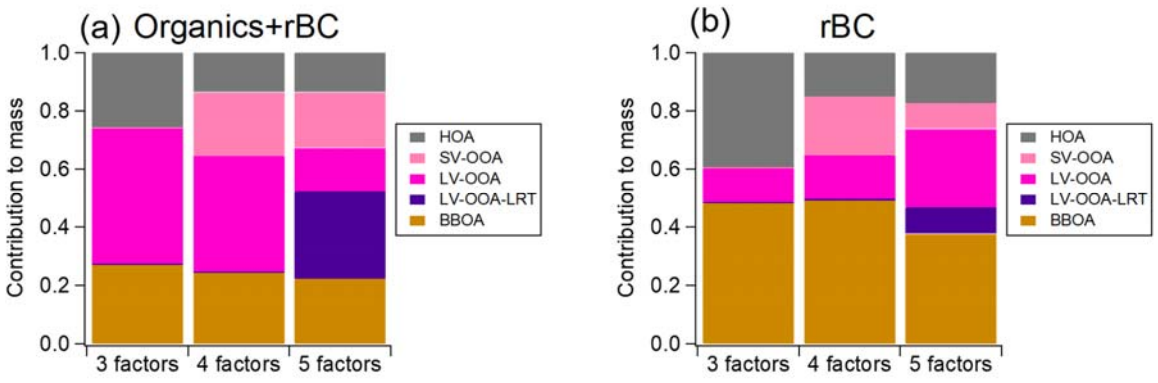

Figure S13. Contribution of 3–5 factors to organics and rBC (a) and rBC (b) at the residential site.

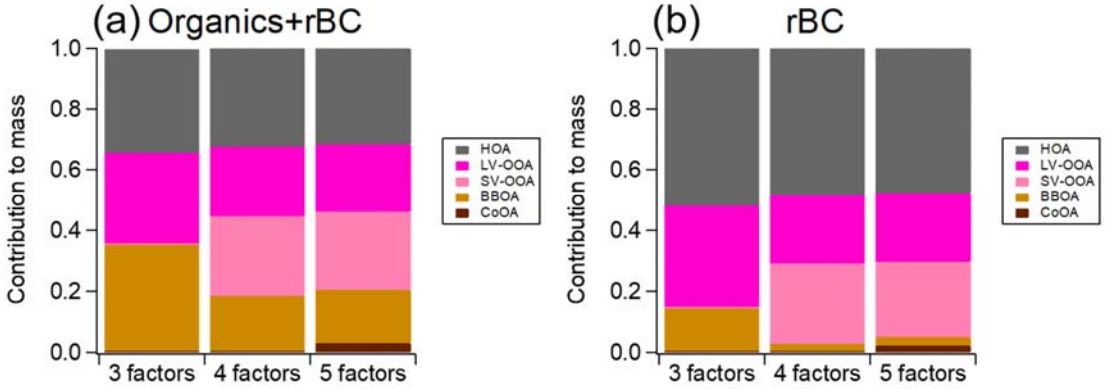

Figure S14. Contribution of 3-5 factors to organics and rBC (a) and rBC (b) at the street canyon.

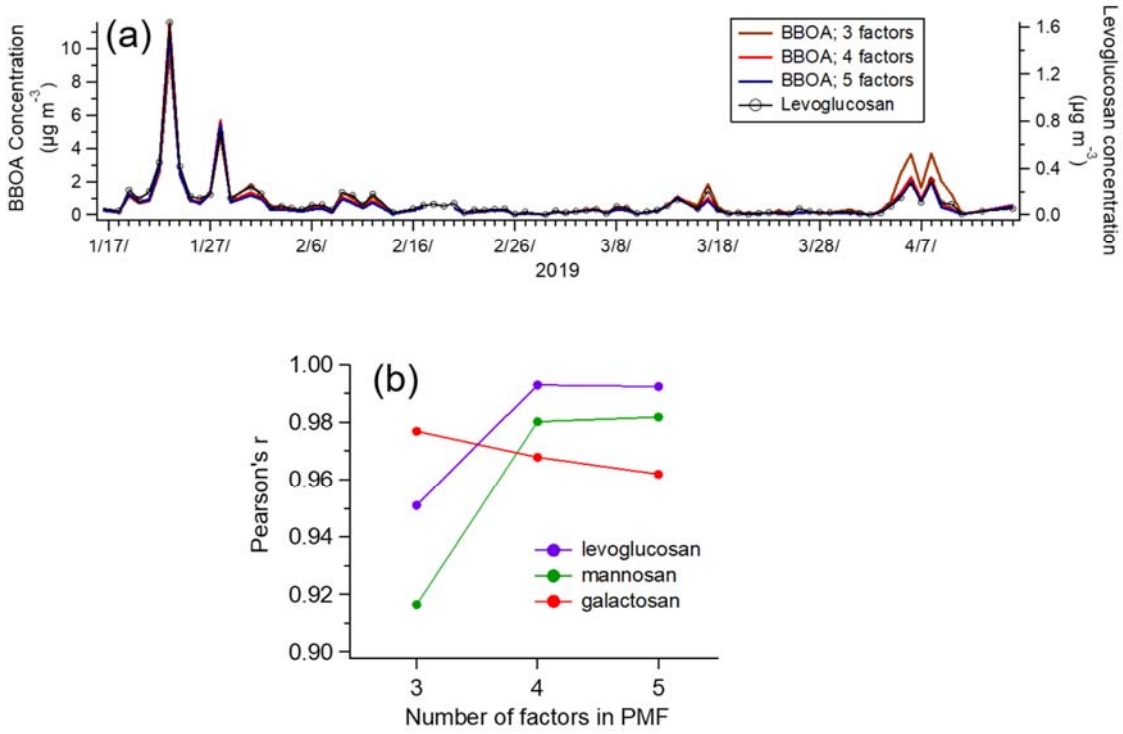

Figure S15. Time series of BBOA in 3–5 factor solutions and levoglucosan analysed from the PM_{10} filter samples (a), and the correlation between the time-series of BBOA in 3–5 factor solutions and levoglucosan, mannosan and galactosan (b). Pearson correlation coefficients.

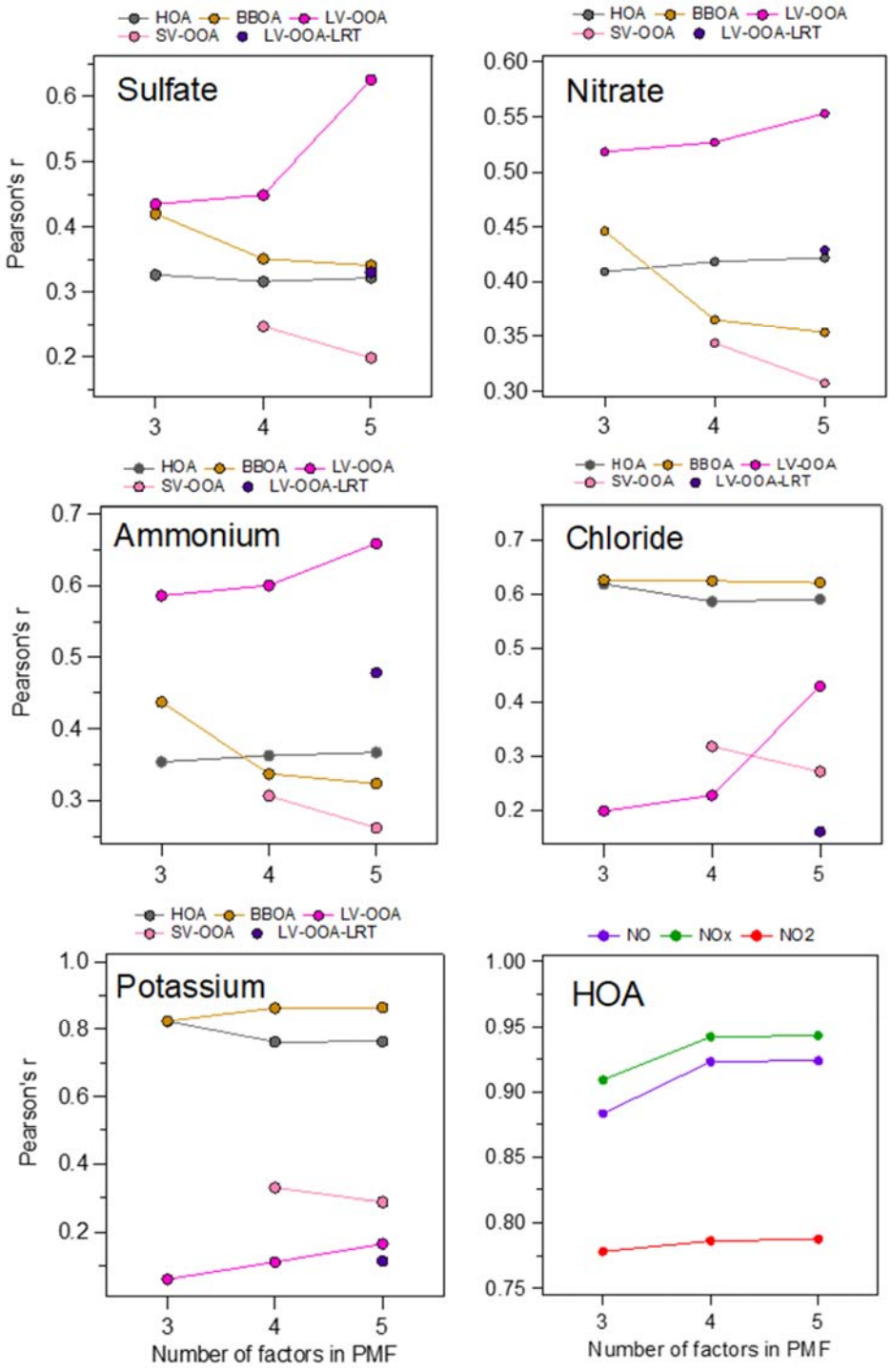

Figure S16. Correlations of the PMF factors with sulfate, nitrate, ammonium, chloride and potassium, and the correlation of HOA with NO, NO_2 and NO in 3–5 factor PMF solutions at the residential site. Pearson correlation coefficients.

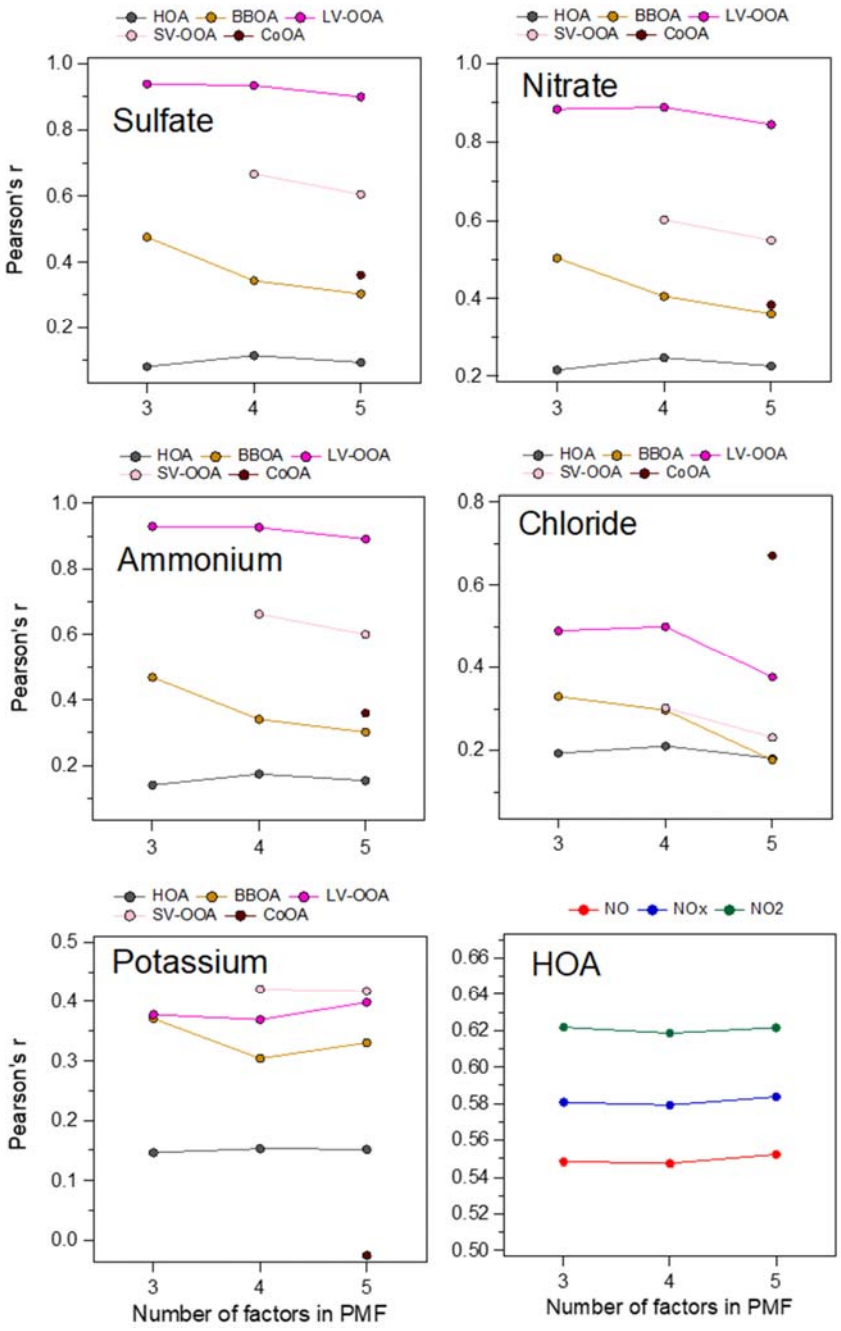

Figure S17. Correlations of the PMF factor with sulfate, nitrate, ammonium, chloride and potassium, and the correlation of HOA with NO_x, NO_2 and NO in 3–5 factor PMF solutions at the street canyon. Pearson correlation coefficients.

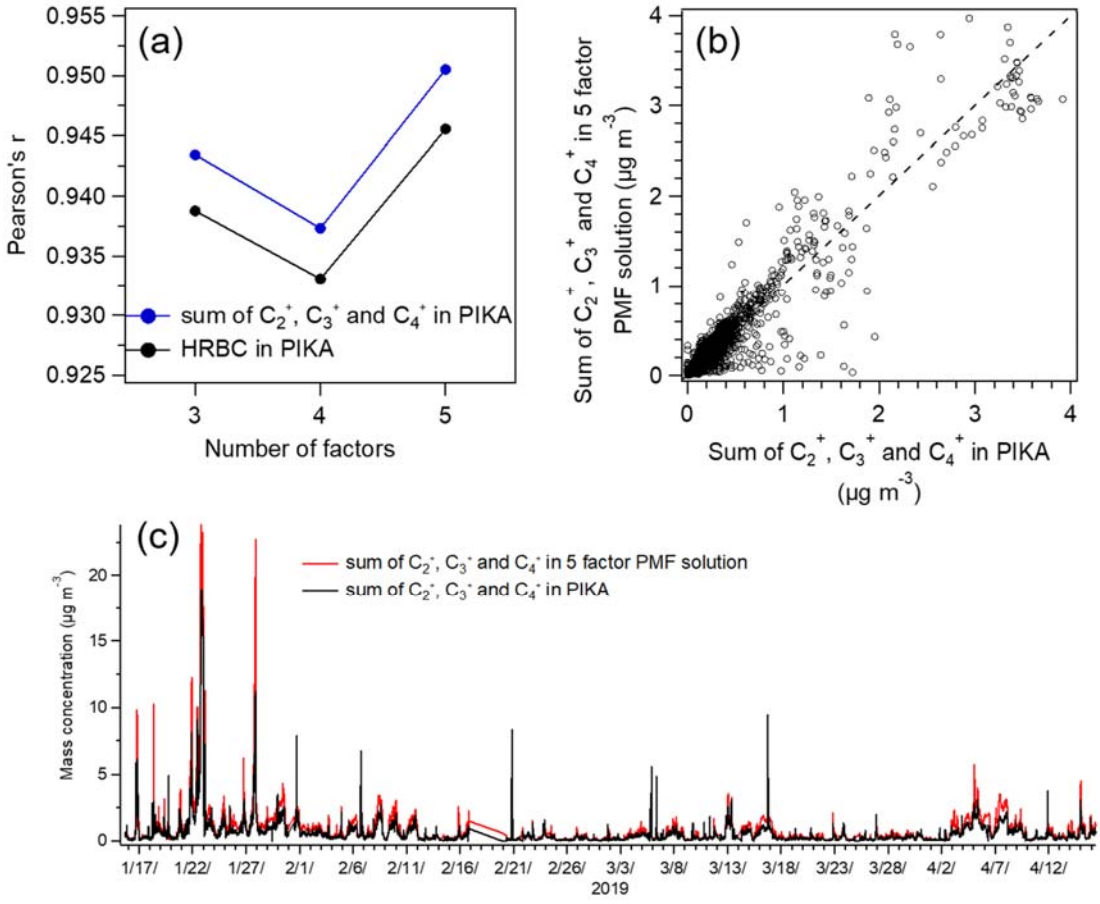

Figure S18. Correlation of the sum of C_2^+, C_3^+ and C_4^+ in 3–5 factor PMF solutions with the sum of C_2^+, C_3^+ and C_4^+ and HRBC in PIKA (a), x,y-plot for the correlation of the sum of C_2^+, C_3^+ and C_4^+ in 5 factor PMF solutions with the sum of C_2^+, C_3^+ and C_4^+ in PIKA (b), and the time-series of the sum of C_2^+, C_3^+ and C_4^+ in 5 factor PMF solutions and in PIKA (c) at the residential site. Dotted line in (b) shows 1:1 line.

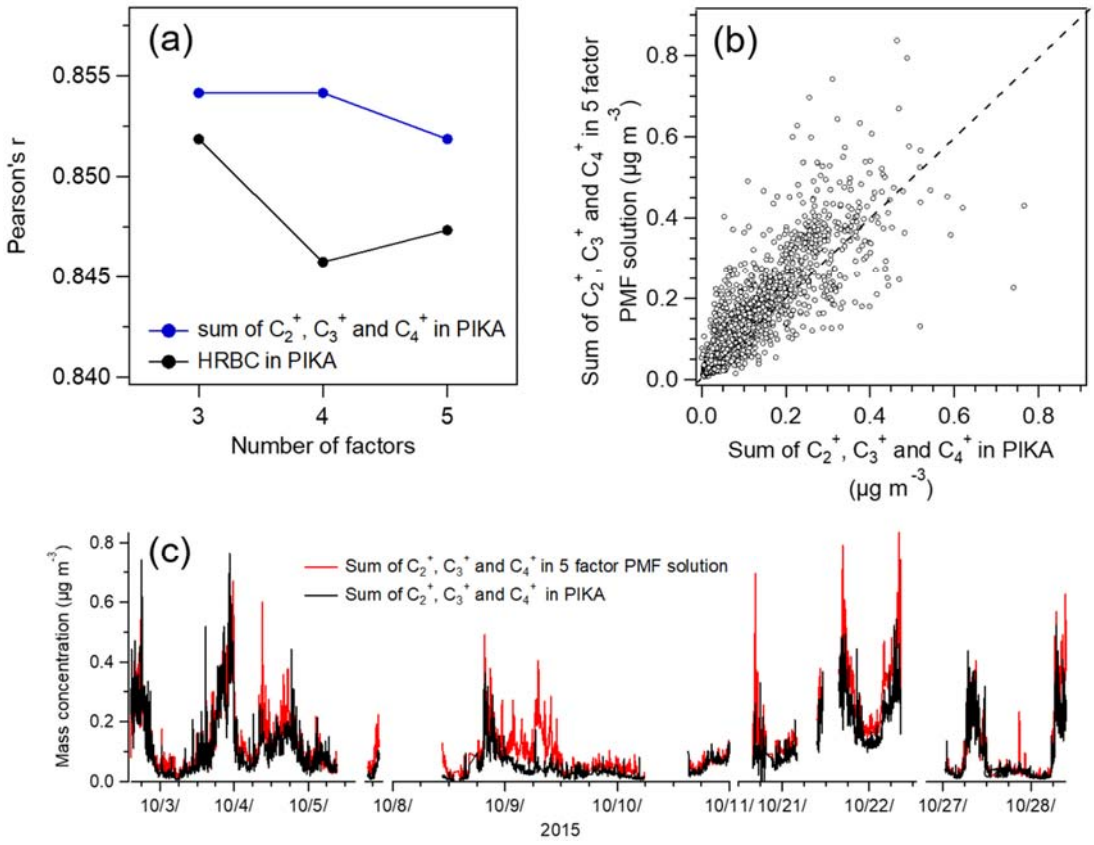

Figure S19. Correlation of the sum of C_2^+, C_3^+ and C_4^+ in 3–5 factor PMF solutions with the sum of C_2^+, C_3^+ and C_4^+ and HRBC in PIKA (a), x,y-plot for the correlation of the sum of C_2^+, C_3^+ and C_4^+ in 5 factor PMF solutions with the sum of C_2^+, C_3^+ and C_4^+ in PIKA (b) and the time-series of the sum of C_2^+, C_3^+ and C_4^+ in 5 factor PMF solutions and in PIKA (c) at the street canyon. Dotted line in (b) shows 1:1 line.

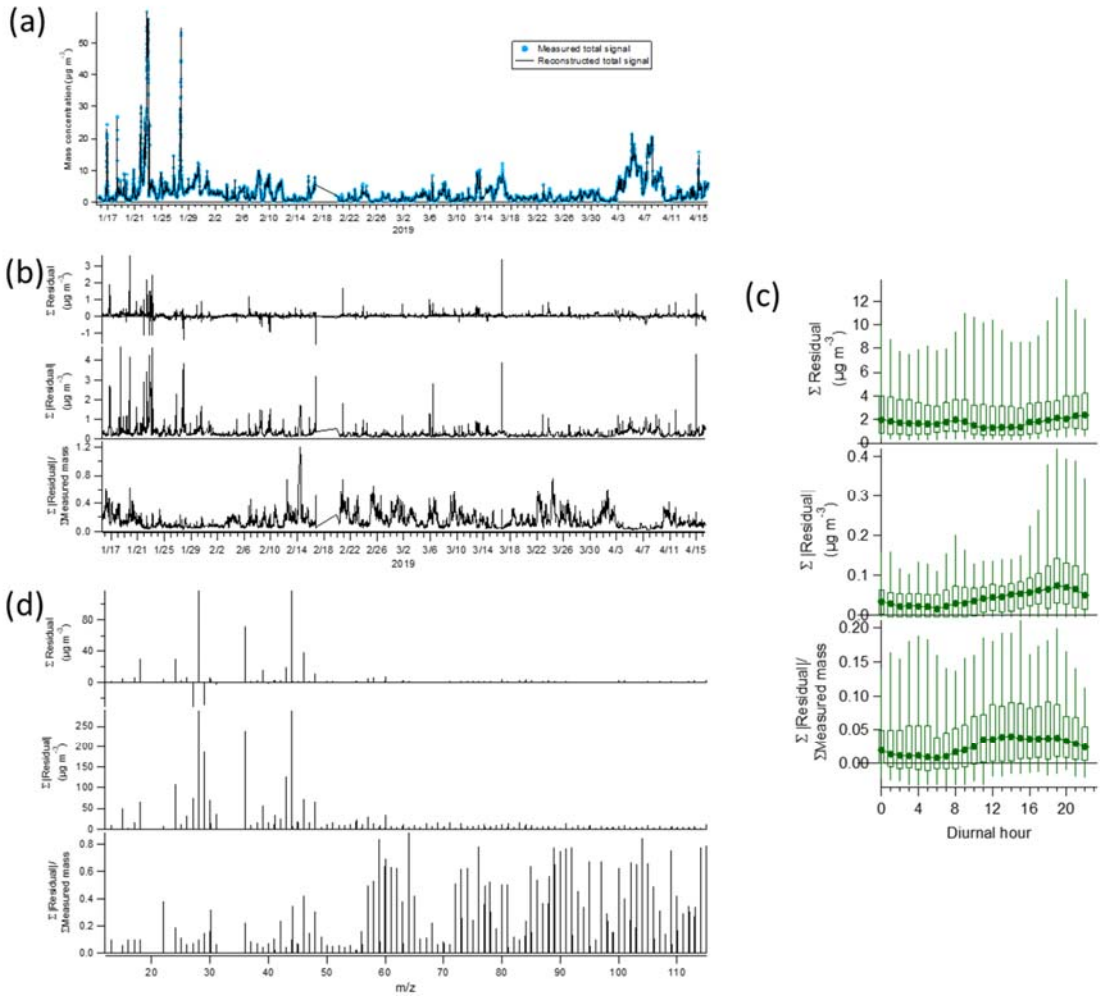

Figure S20. Analysis of the residuals at the residential site for the five factor PMF solution. Time series of the mass concentrations of measured and reconstructed Organics+rBC (a), time series of residuals (b), diurnal variation of residuals (c), and the residuals in the mass spectra (c). In (b)–(d) the residuals are presented as total residual, total absolute residual and absolute residual normalized by total signal over the whole measurement period. In (c) medians are denoted by markers, 25–75% by boxes and the whole range of values by bars.

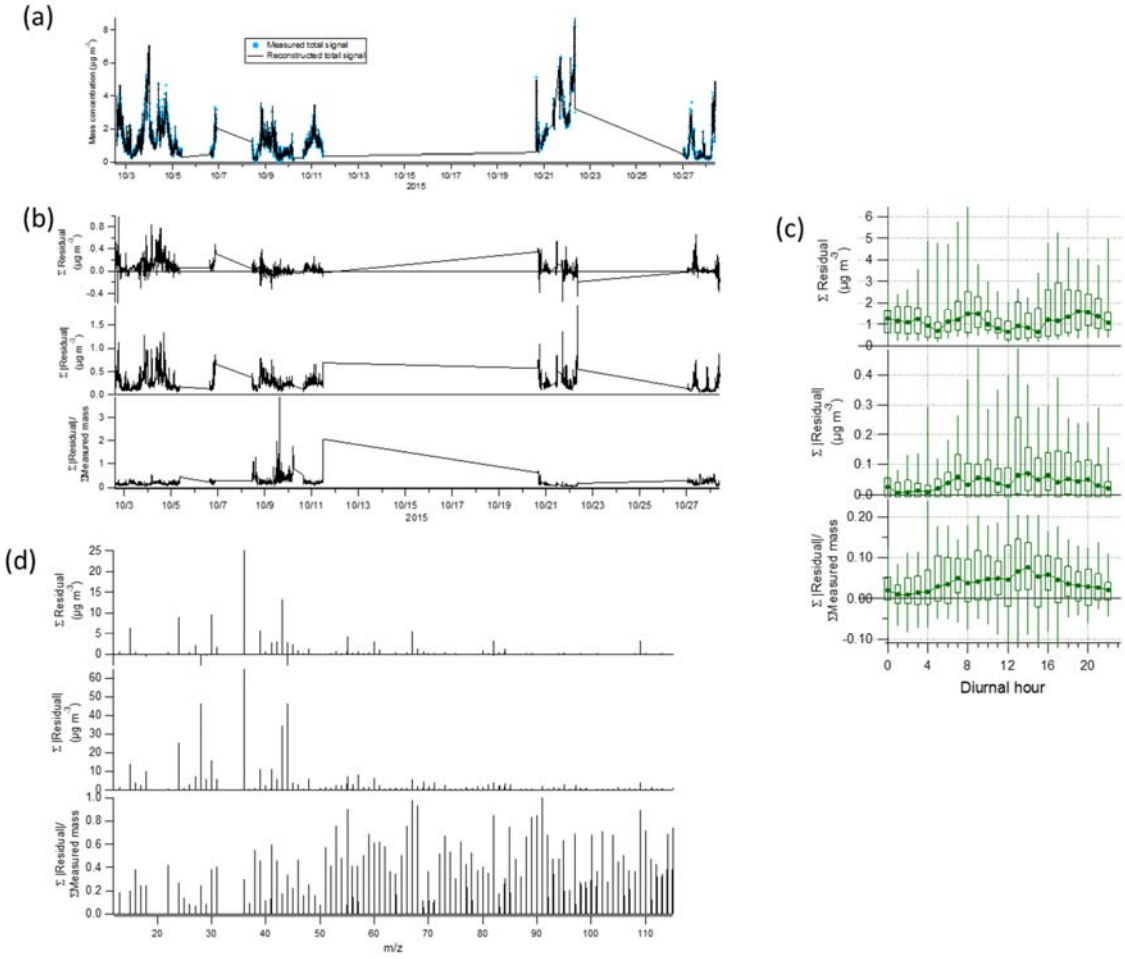

Figure S21. Analysis of the residuals at the street canyon for the three factor PMF solution. Time series of the mass concentrations of measured and reconstructed Organics+rBC (a), time series of residuals (b), diurnal variation of residuals (c), and the residuals in the mass spectra (c). In (b)-(d) the residuals are presented as total residual, total absolute residual and absolute residual normalized by total signal over the whole measurement period. In (c) medians are denoted by markers, 25-75% by boxes and the whole range of values by bars.

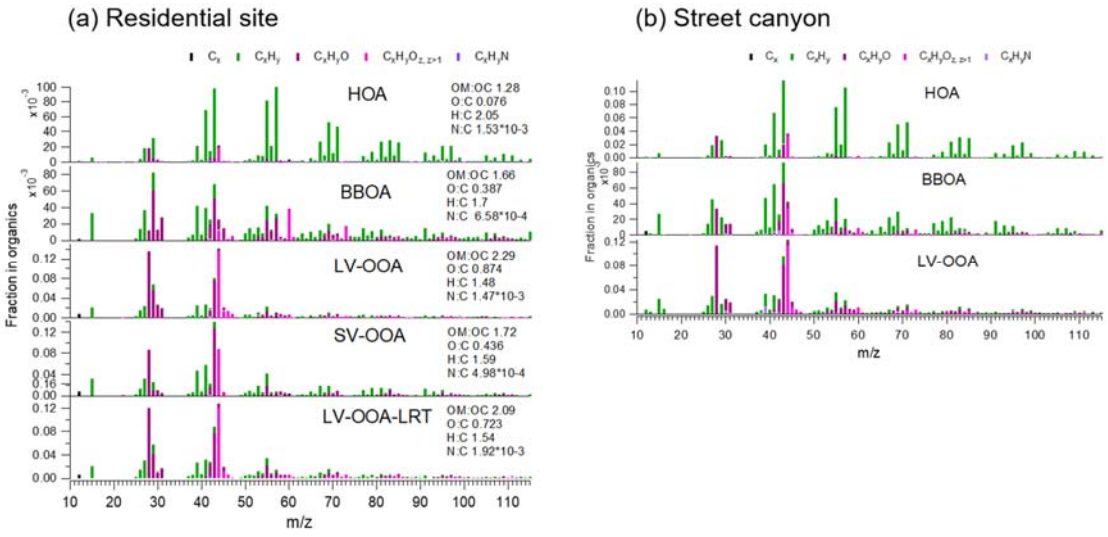

Figure S22. Five-factor PMF solution at the residential site (a) and three-factor PMF solution at the street canyon (b) for organics. Colors in the mass spectra represent different types of organic fragments.

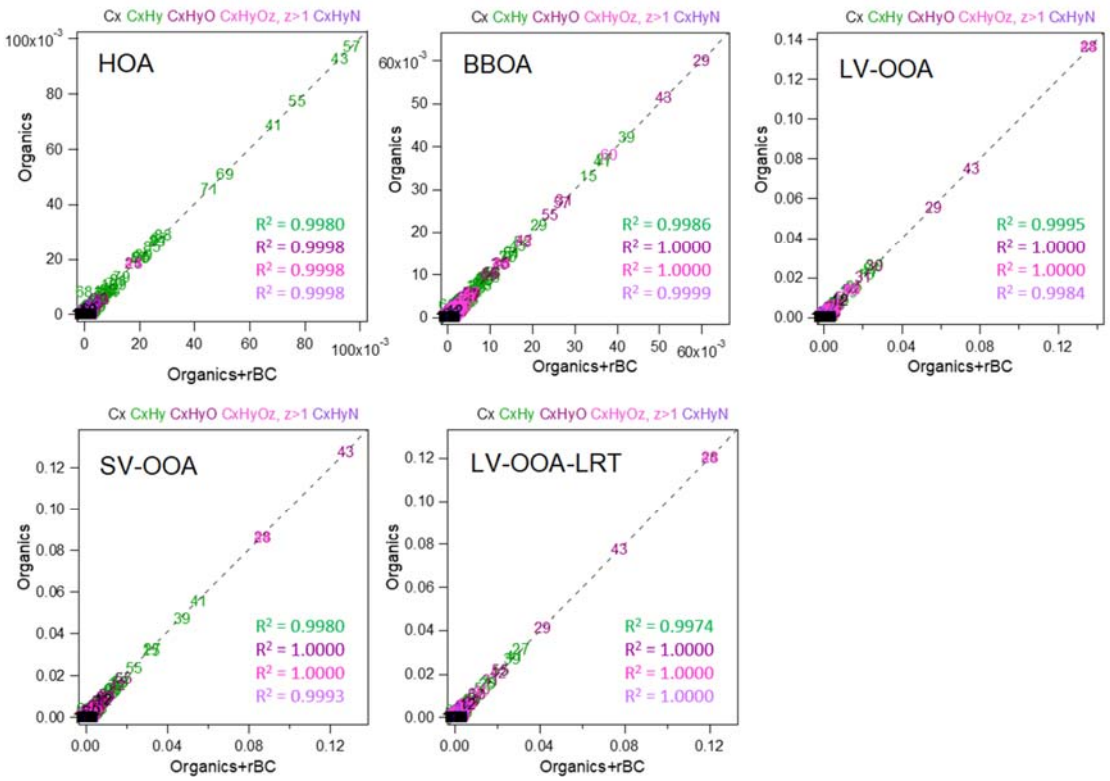

Figure S23. Comparison of mass spectra between the PMF solution with Organics+rBC and organics for five factor solution at the residential site. x-and y-axis units are fraction in organics. R^2 is the coefficient of determination in linear regression. Dotted line shows 1:1 line. Colors represent different types of organic fragments.

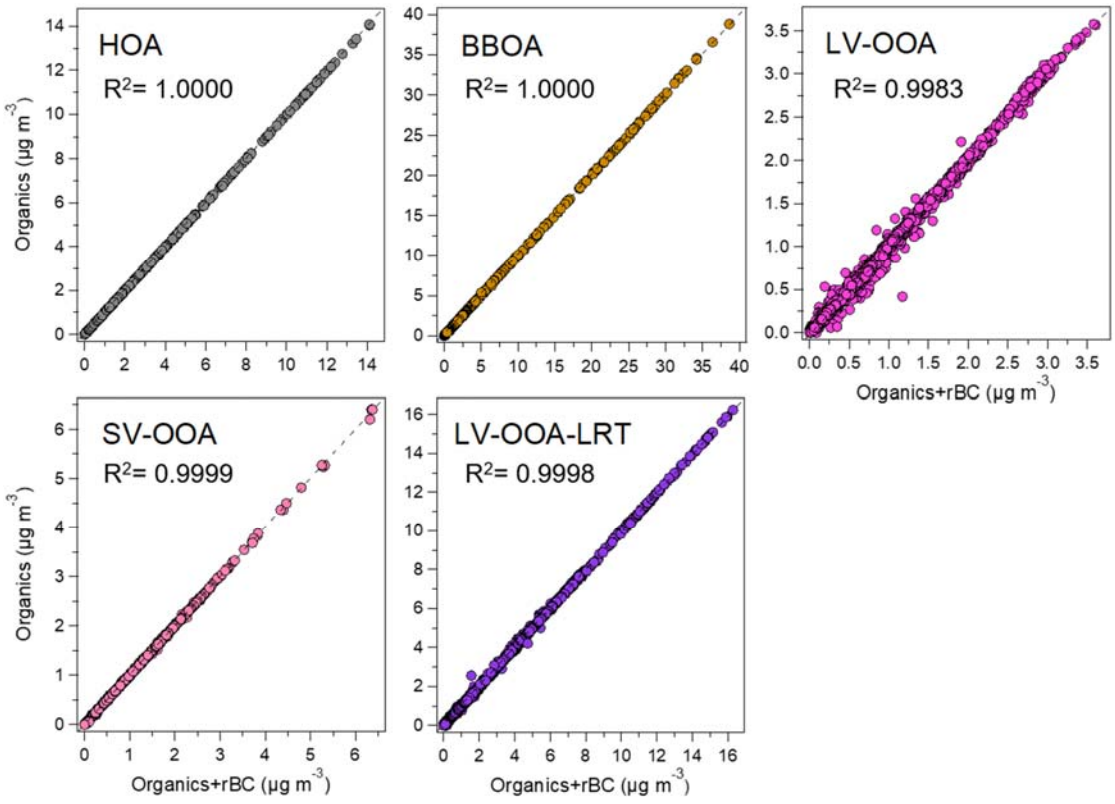

Figure S24. The comparison of time series between the PMF solution with Organics+rBC and organics for five factor solution at the residential site. R^2 is the coefficient of determination in linear regression. Dotted line shows 1:1 line.

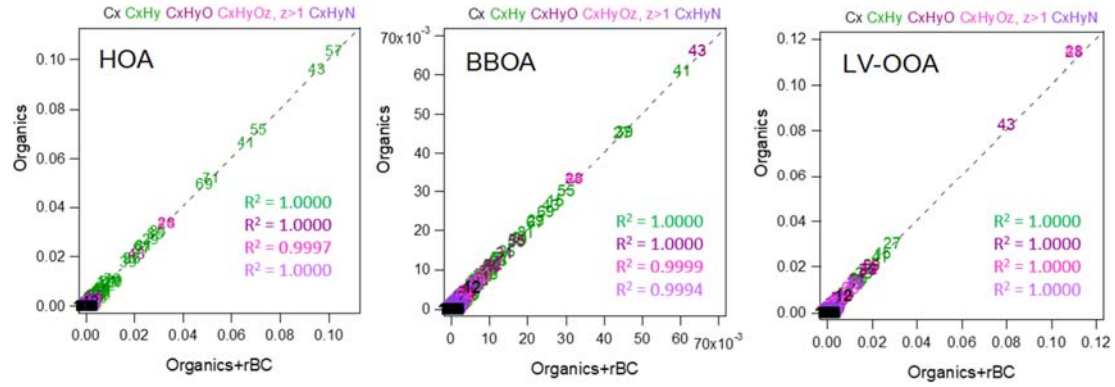

Figure S25. Comparison of mass spectra between the PMF solution with Organics+rBC and organics for three factor solution at the street canyon. x-and y-axis units are fraction in organics. R^2 is the coefficient of determination in linear regression. Dotted line shows 1:1 line. Colors represent different types of organic fragments.

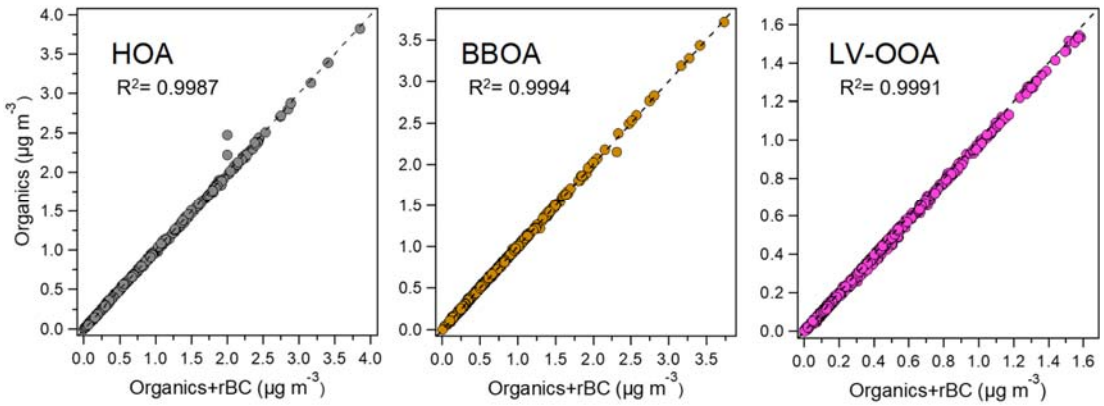

Fig. S26. The comparison of time series between the PMF solution with Organics+rBC and organics for three factor solution at the street canyon. R^2 is the coefficient of determination in linear regression. Dotted line shows 1:1 line.

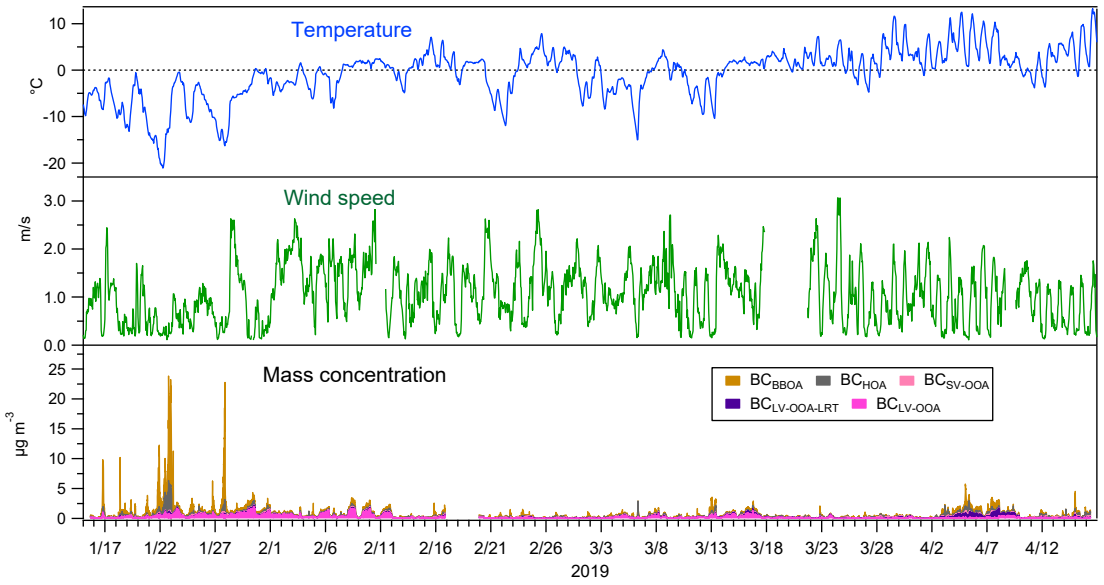

Figure S27. Time-series of ambient temperature, wind speed and the PMF factors at the residential area from January 16 to April 16 2019.

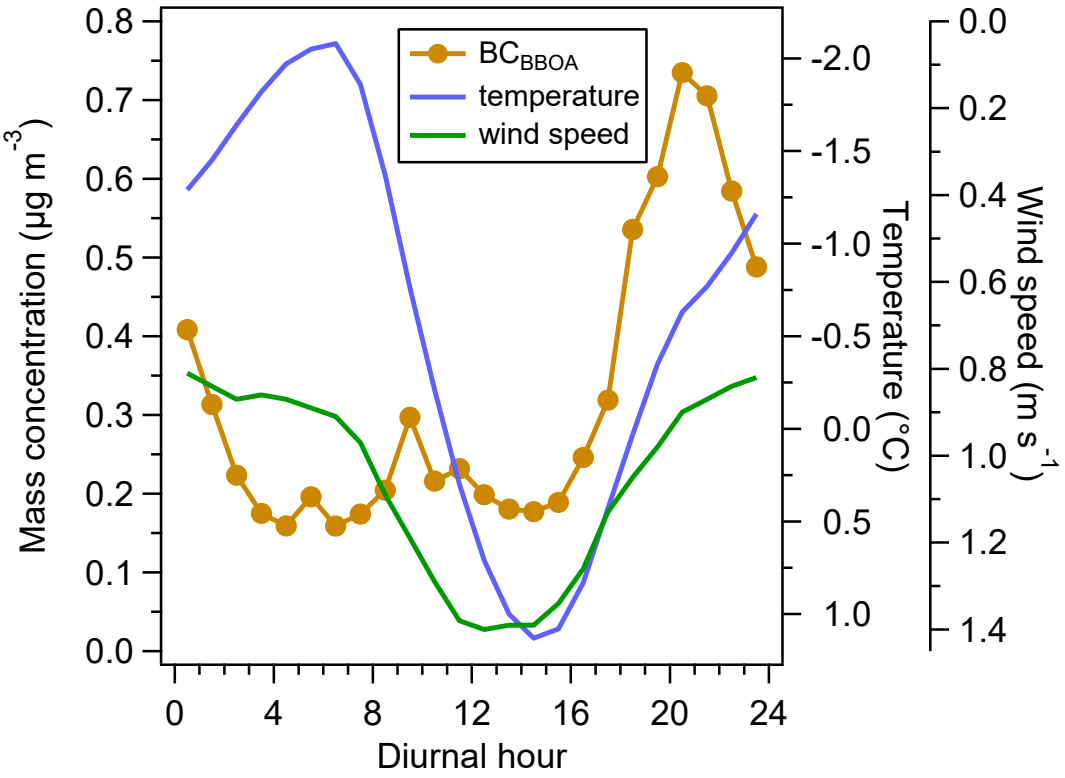

Figure S28. Diurnal variation of BC_{BBOA}, ambient temperature and wind speed at the residential site. Note that the values shown in left and right y-axes are on opposite direction.

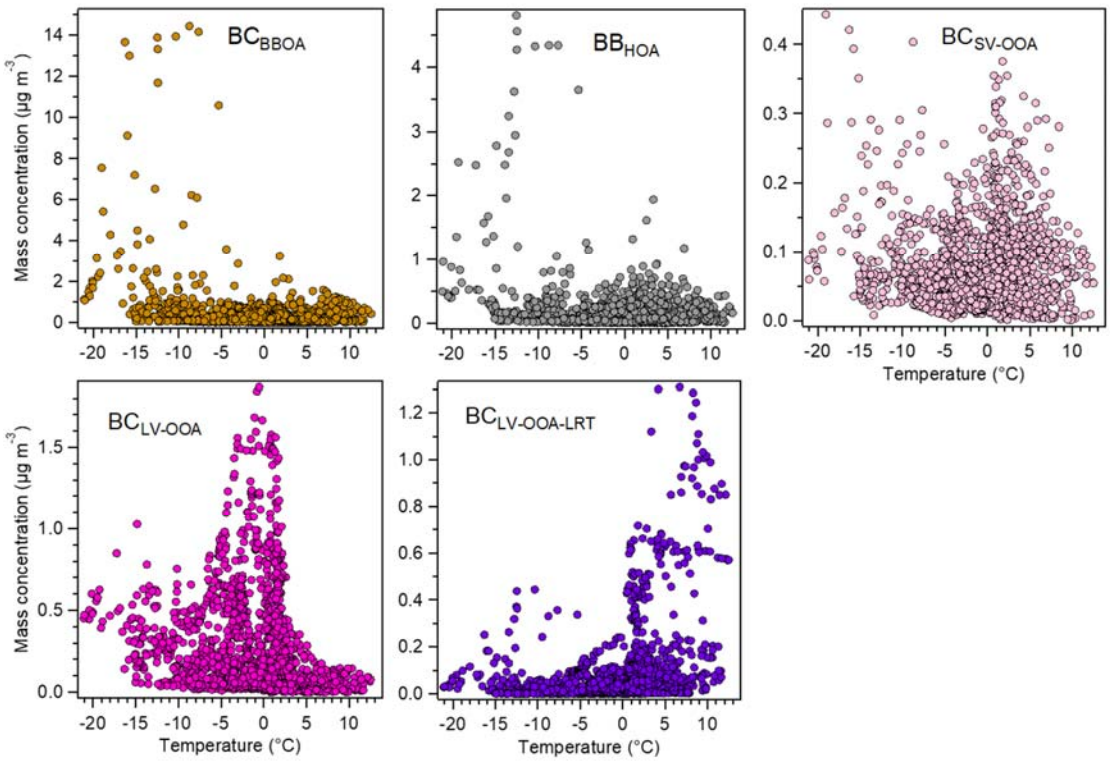

Figure S29. Correlation of the mass concentrations of the PMF factors with ambient temperature.

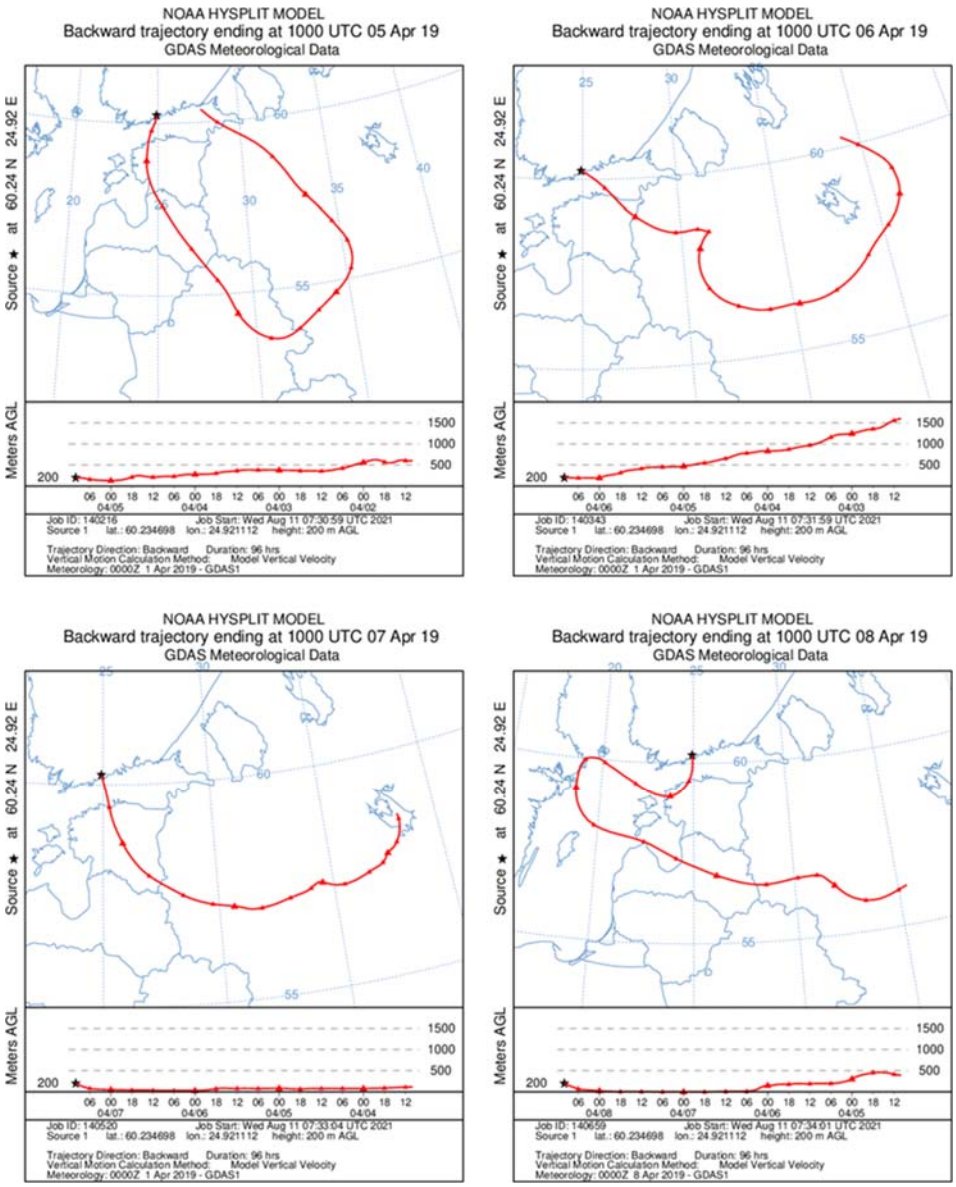

Figure S30. Calculated 96-hour back trajectories for four days (5–8 April 2019, 200 m) during the LRT period at the residential site. Calculated at 12:00 (local time). Trajectories were calculated using the NOOA HYSPLIT model (Stein et al. 2015; Rolph et al. 2017).

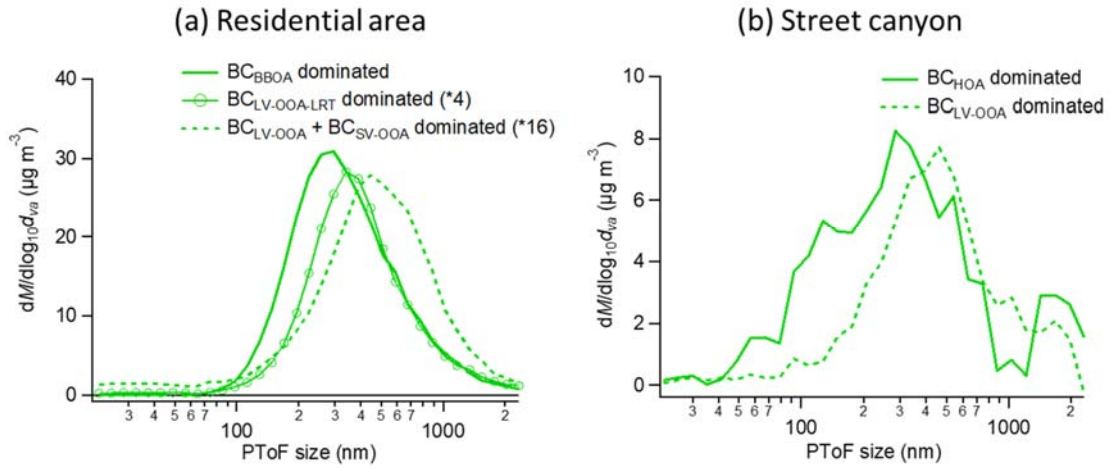

Figure S31. Mass size distribution of organics at the residential area (a) and street canyon (b). Average mass size distributions during the periods when BC_{BBOA}, $BC_{LV\text{-}OOA\text{-}LRT}$ or the sum of $BC_{LV\text{-}OOA}$ and $BC_{SV\text{-}OOA}$ dominated total BC concentration (a), and average mass size distributions during the periods when BC_{HOA} or $BC_{LV\text{-}OOA}$ dominated total BC concentration (b).

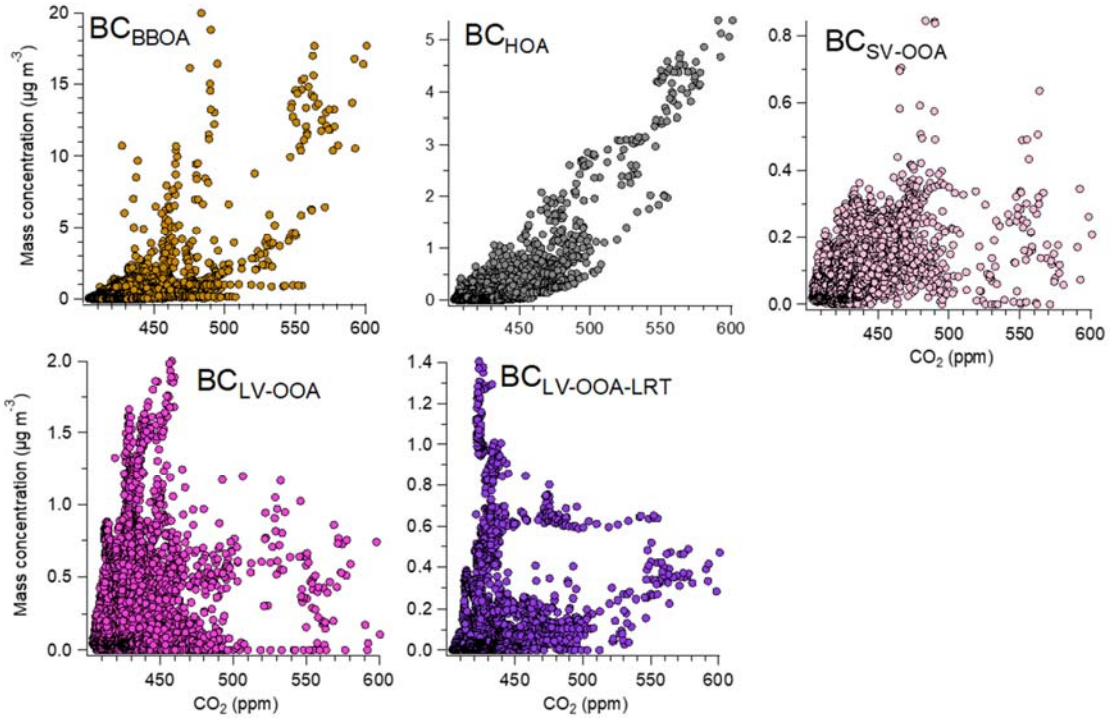

Figure S32. Correlation of PMF factors with the measured CO_2 concentrations at the residential site.

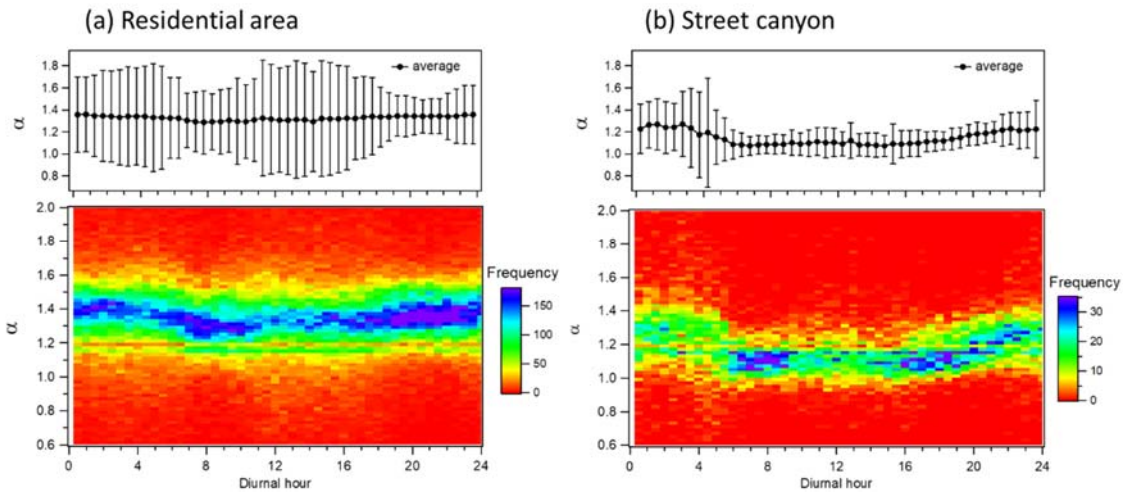

Figure S33. Diurnal variation of absorption Ångström exponents at the residential area (a) and street canyon (b). Average (± stdev) and the probability distribution function (1-min time resolution data).

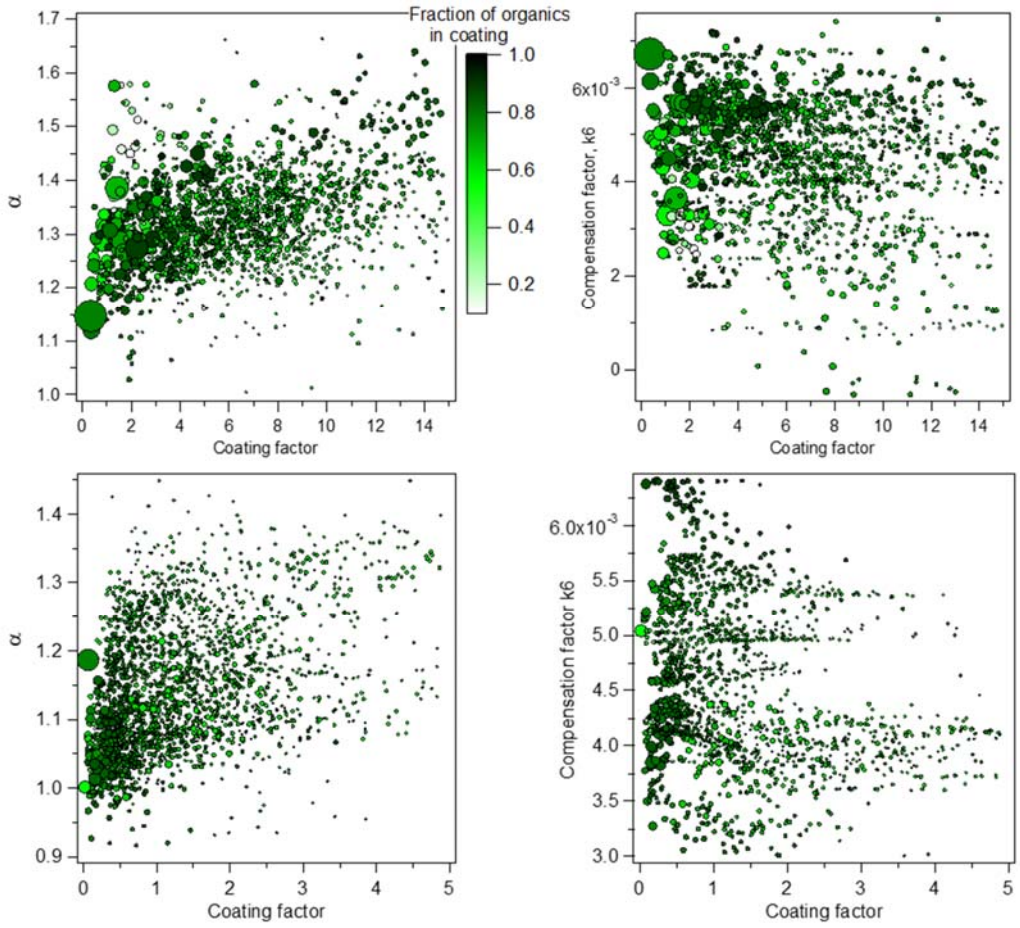

Figure S34. Absorption Ångström exponent (α) and compensation factor at 880 nm (k6) plotted against the coating factor at the residential (a–b) and street canyon (c–d) site. α was calculated as the ratio of 470 nm to 950 nm. Color presents the contribution of organics in the coating. Marker size displays ambient BC concentration.

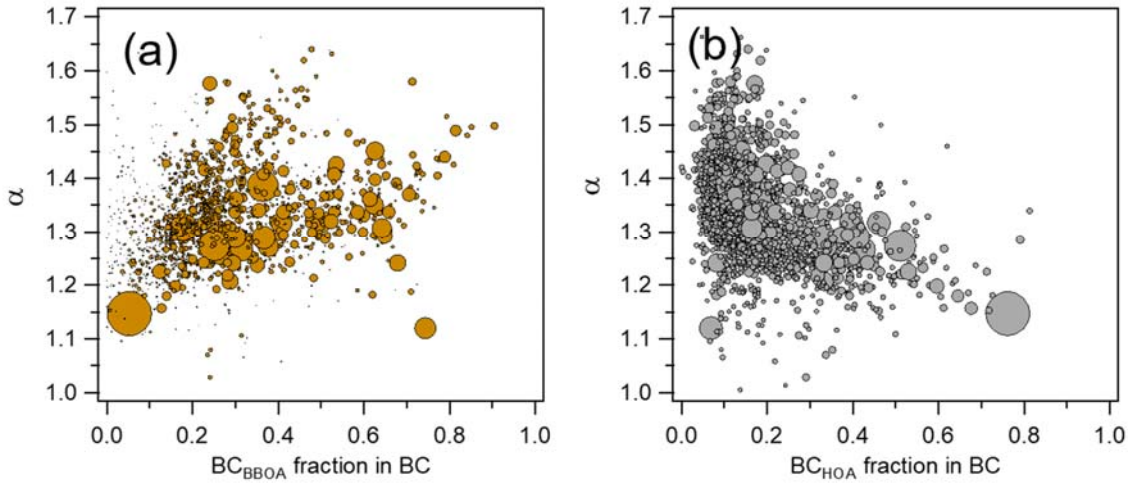

Figure S35. Absorption Ångström exponents plotted against BC_{BBOA} (a) and BC_{HOA} (b) fractions in total BC at the residential site. α was calculated as a ratio of 470 nm to 950 nm. Marker size displays BC concentration.

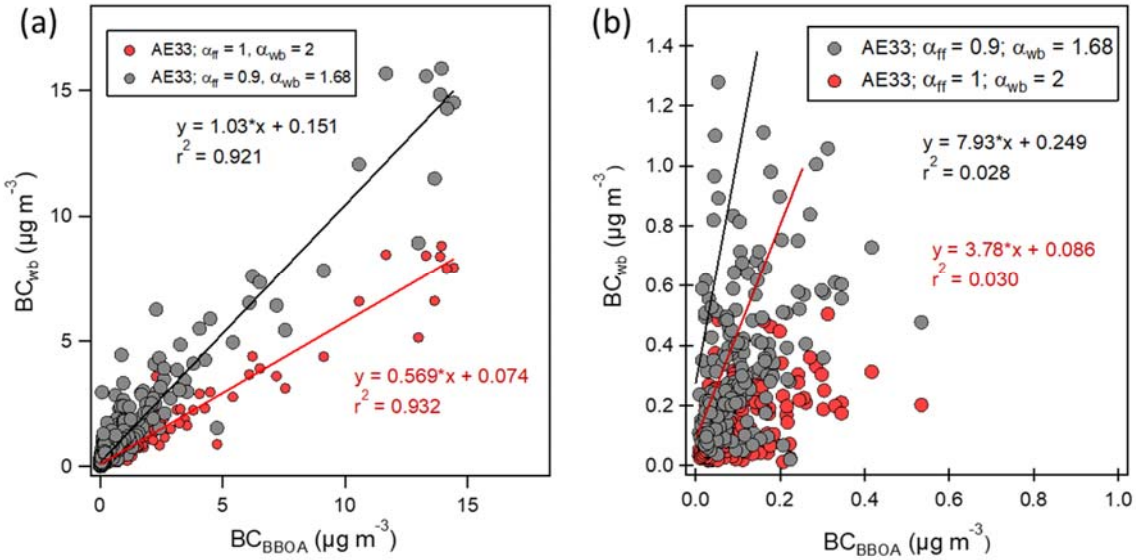

Figure S36. Comparison of BC_{wb} and BC_{BBOA} concentrations at the residential area (a) and street canyon (b) with a line fitting. BC_{wb} with the aethalometer model was calculated by using $\alpha_{ff} = 0.9$ and $\alpha_{wb} = 1.68$, and $\alpha_{ff} = 1$ and $\alpha_{wb} = 2$. 1-hour time resolution.

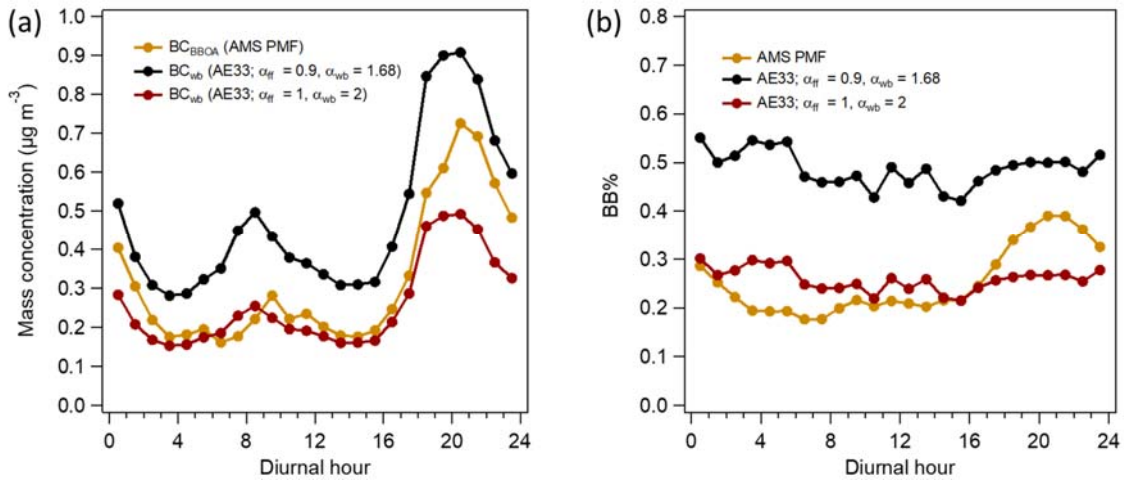

Figure S37. Average diurnal trends for BC_{BBOA} and BC_{wb} (a) and BB% (b) at the residential site. BC_{wb} and BB% were calculated by using $\alpha_{ff} = 0.9$ and $\alpha_{wb} = 1.68$, and $\alpha_{ff} = 1$ and $\alpha_{wb} = 2$.

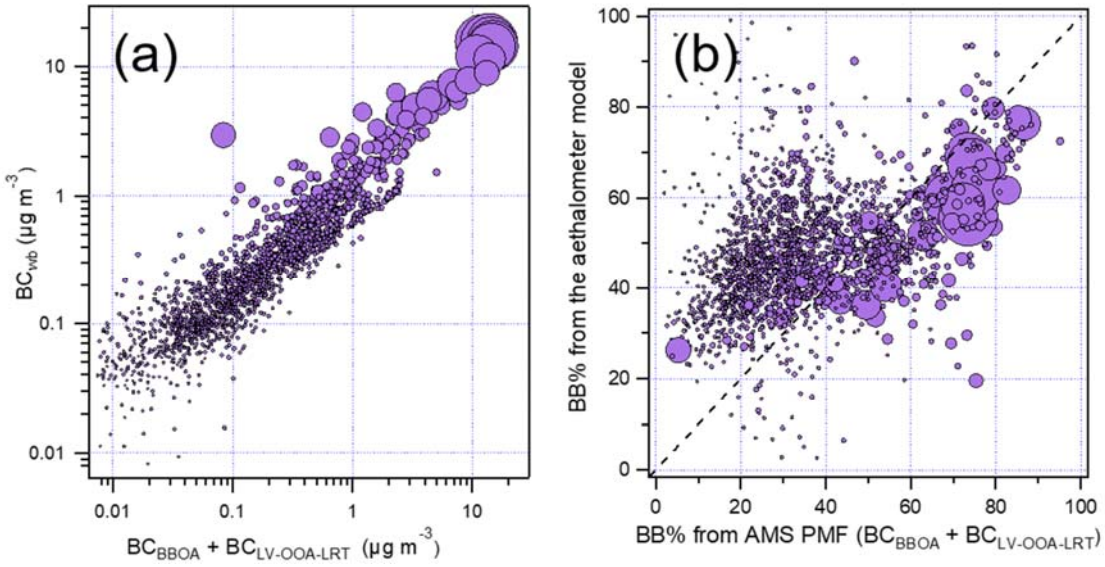

Figure S38. The comparison of BC_{wb} from the aethalometer model and the sum of BC_{BBOA} and $BC_{LV\text{-}OOA\text{-}LRT}$ from AMS-PMF at the residential site. Concentrations (a) and BB% (b). BC_{wb} was calculated by using $\alpha_{ff} = 0.9$ and $\alpha_{wb} = 1.68$. 1-hour time-resolution. Marker size illustrates the total BC concentration. Dotted line in (b) shows 1:1 line.

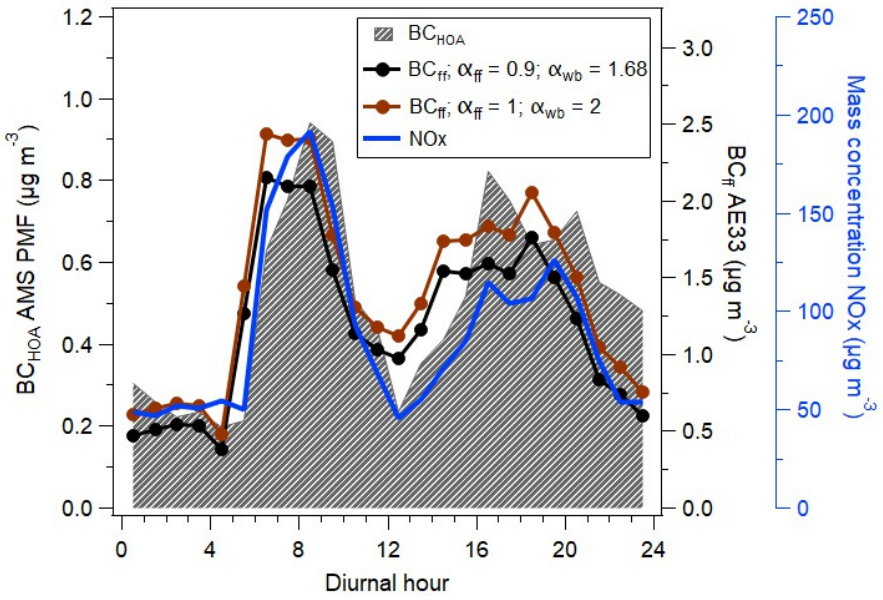

Figure S39. The comparison of diurnal patterns of BC_{ff} from the aethalometer model and BC_{BBOA} from AMS-PMF at the street canyon. BC_{ff} was calculated by using $\alpha_{ff} = 0.9$ and $\alpha_{wb} = 1.68$. Also the diurnal pattern of NOx is presented.

References

Rolph, G., Stein, A., Stunder, B.: Real-time Environmental Applications and Display sYstem: READY. Environmental Modelling & Software 95, 210–228, 2017.

Stein, A. F., Draxler, R.R, Rolph, G. D., Stunder, B. J. B., Cohen, M. D., Ngan, F.: NOAA's HYSPLIT atmospheric transport and dispersion modeling system. Bull. Amer. Meteor. Soc. 96, 2059—2077, 2015.